

Two or four Neoproterozoic glaciations?

Martin J. Kennedy* } Department of Earth and Space Sciences and Institute of Geophysics and
 Bruce Runnegar } Planetary Physics, University of California, Los Angeles, California 90095-1567
 Anthony R. Prave } School of Geography and Geosciences, University of St. Andrews, Fife KY16 9ST, Scotland
 K.-H. Hoffmann } Geological Survey of Namibia, P.O. Box 2168, Windhoek, Namibia
 Michael A. Arthur } Department of Geosciences and Earth System Science Center, Pennsylvania State University,
 University Park, Pennsylvania 16802

ABSTRACT

A thick Neoproterozoic carbonate and glaciogenic succession of the southern Congo craton has yielded $\delta^{13}\text{C}$ and $^{87}\text{Sr}/^{86}\text{Sr}$ records through the later Cryogenian (ca. 750–600 Ma) and earlier part of the Terminal Proterozoic (ca. 600–570 Ma). Sizeable negative $\delta^{13}\text{C}$ excursions (to less than –5‰) occur above each of two glacial intervals and the $^{87}\text{Sr}/^{86}\text{Sr}$ values of marine carbonates shift from ~ 0.7072 to ~ 0.7079 at the upper glacial level. These geochemical constraints provide a Marinoan (younger Varanger) age for the upper glacial interval, previously regarded as a second phase of the Sturtian glaciation. The $\delta^{13}\text{C}$ record from the Congo craton is therefore incompatible with recent global $\delta^{13}\text{C}$ syntheses that have identified four or more separate ice ages during the Neoproterozoic. A cladistic analysis of geologic and geochemical characters of 12 Neoproterozoic glacial deposits identifies two distinct groups that are found in a consistent stratigraphic order whenever two glacial units occur within a single succession. We use $\delta^{13}\text{C}$ and $^{87}\text{Sr}/^{86}\text{Sr}$ records from the Congo craton and other key successions to test the null hypothesis that there were only two global glaciations (Sturtian and Marinoan) during the Neoproterozoic. Placing the GSSP (global stratotype section and point) for the base of the Terminal Proterozoic within or just above a cap carbonate of the younger (Marinoan) glaciogenic succession would confine all known Neoproterozoic glaciations to the Cryogenian. The rapid shift in marine $^{87}\text{Sr}/^{86}\text{Sr}$ to more radiogenic values during the Marinoan glaciation is opposite that predicted by the snowball Earth scenario which calls for continental runoff to cease during glaciation, resulting in a shift to less radiogenic values.

INTRODUCTION

Terminal Proterozoic glacial intervals are closely linked with excursions to strongly negative carbon isotope ratios ($\delta^{13}\text{C} \leq -4\text{‰}$ relative to the PDB [Peedee belemnite] standard; Knoll et al., 1986; Kaufman et al., 1997). The occurrence of these deposits on basinal to interbasinal scales, their association with marine carbon isotope excursions, and paleomagnetic evidence for low-latitude glaciation (Schmidt and Williams, 1995), all suggest that these deposits record global climatic events and provide evidence of Earth's most extreme ice ages (Harland, 1964; Kirschvink, 1992; Hoffman et al., 1998a, 1998b). Although no known Neoproterozoic succession contains more than two glacial intervals, as many as five successive ice ages have been proposed (Kaufman et al., 1997; Hoffman et al., 1998a; Saylor et al., 1998). Evidence for additional Neoproterozoic glaciations comes from the integration of lithostratigraphic, paleontologic, and chemostratigraphic records from sections in Spitsbergen, Canada, Australia, and the Congo and Kalahari cratons of Namibia (Kaufman et al., 1997, and references therein).

Here, we assess this global synthesis by using detailed $\delta^{13}\text{C}$ and $^{87}\text{Sr}/^{86}\text{Sr}$ records from the

Congo craton, where a thick succession (>1000 m) of platform and slope carbonates includes two Neoproterozoic glacial horizons (Hoffmann and Prave, 1996; Hoffman et al., 1998a, 1998b). We then relate these records to the global setting by (1) demonstrating by means of a cladistic analysis that 12 well-known Neoproterozoic glaciogenic deposits fall into two separate groups, which we term "Sturtian" and "Marinoan," (2) showing that a substantial rise in oceanic $^{87}\text{Sr}/^{86}\text{Sr}$ (by 0.0007) follows the upper (Marinoan) glacial interval, and (3) highlighting the Congo craton succession as one of the least ambiguous records of chemostratigraphic and geologic events across the Cryogenian–Terminal Proterozoic boundary. In addition, we use new $\delta^{13}\text{C}$ and $^{87}\text{Sr}/^{86}\text{Sr}$ data to assess the "snowball Earth" scenario of Hoffman et al. (1998b).

LITHOSTRATIGRAPHY OF THE CHUOS AND GHAUB GLACIATIONS

Two glacial intervals, each overlain by lithologically distinctive cap carbonates, are present within platform and ramp carbonates along the southern margin of the Congo craton (Hoffmann and Prave, 1996; Hoffman et al., 1998a, 1998b). Iron-rich diamictites within the lower glacial interval (Chuoss Formation; Fig. 1) are overlain abruptly by a transgressive lower cap carbonate (Rasthof Formation) composed of black, organic-

rich laminites and peloidal grainstones. The lowest few meters are mechanically laminated; they grade upward into a thick succession of anastomosing and rhythmic laminae, distinctive decimeter-scale rollup structures, and slumped and overhanging domes of microbial origin. These microbialites shoal upward to a well-developed karst surface. The remaining interglacial succession (Gruis and Ombaatjie Formations) consists of upward-shoaling carbonate units that culminate in exposure surfaces and local erosion (Prave, 1996).

Glaciogenic facies of the Ghaub Formation fill valleys incised into the underlying carbonate platform along a regionally persistent erosion surface. Where diamictite is absent along this surface, transgressive carbonates, including a distinctive tubestone marker bed, are present. This marker bed is characterized by long, vertical, tubular structures (Hegenberger, 1987; Hoffmann and Prave, 1996; Hoffman et al., 1998b) defined by millimeter-scale, meniscus-like laminae that are continuous from intertube regions through the tube structures, implying a mechanical rather than a biological (stromatolitic) origin. Elsewhere, the diamictite is abruptly overlain by thin, tan-colored dolostone that is organic lean, laminated, microcrystalline, and has syndimentary, cement-lined sheet cracks. Buckled, marine-cemented beds like those described by Kennedy (1996) and relict aragonite crystal fans are also present (Hoffman et al., 1998a). The tubestones and dolostones (Keilberg Member) are interbedded over several meters with the base of the Maieberg Formation, a thick highstand succession (>300 m) of deeper water, hemipelagic, rhythmite-marl event beds, interclastic breccias, and nodular siltstones. These are succeeded by ooid grainstones, stromatolites, and traction-bedded carbonates that overlie a regional erosion surface (sequence boundary) at the top of the Maieberg Formation (Prave, 1996; Hoffman et al., 1998a, 1998b). The Maieberg Formation and the overlying shallow water deposits of the Elandshoek and Huttenberg Formations are locally truncated beneath a regional angular unconformity (base of Mulden Group).

CHEMOSTRATIGRAPHY

Carbonate samples were collected from the top of the lower glacial interval (Chuoss Forma-

*Current address: Exxon Production Research Company, P.O. Box 2189, Houston, Texas 77252-2189.

Data Repository item 9887 contains additional material related to this article.

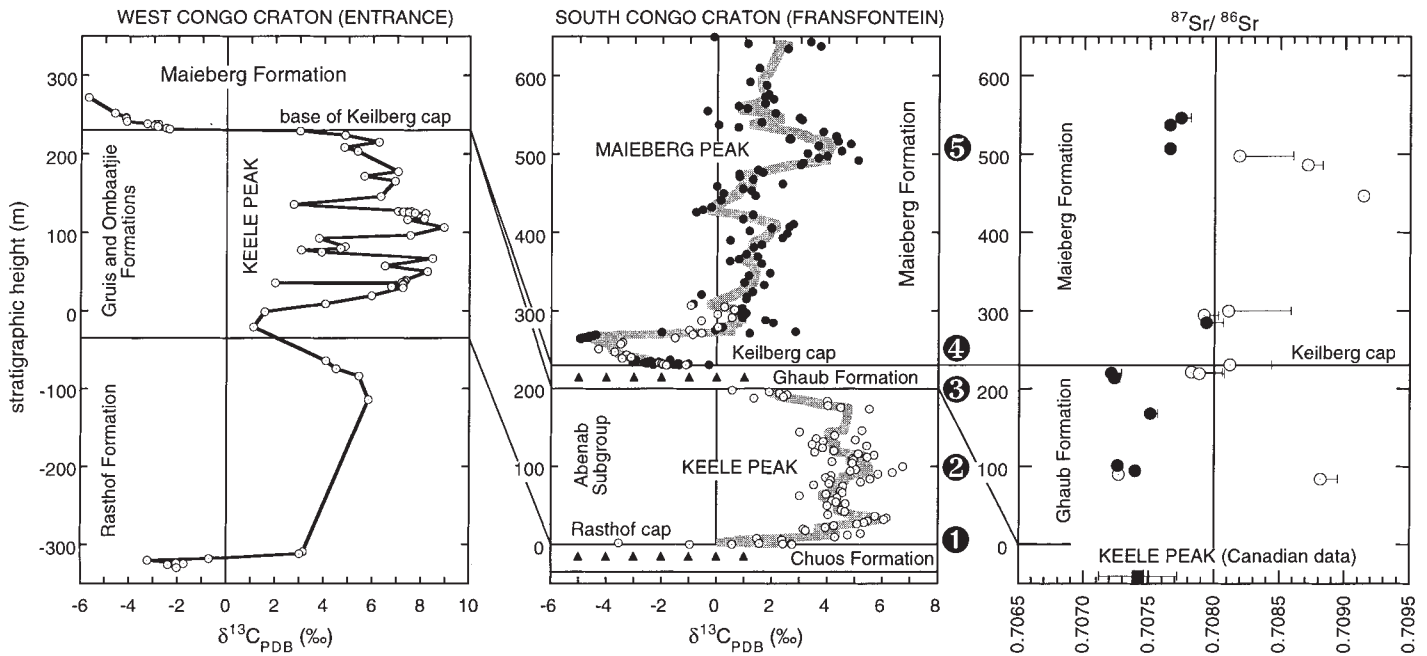


Figure 1. Strontium and carbon isotope data from three sections on the Congo craton. Left panel, Entrance-Hoanib River (13.9°E, 19.2°S); center panel, Fransfontein (15°E, 20.2°S) and Duurwater, 15 km to east (open circles); right panel, $^{87}\text{Sr}/^{86}\text{Sr}$ data. Gray curves are five-point weighted averages; circled numbers are benchmarks explained in text. In right panel, filled symbols are $\delta^{18}\text{O} > -7\text{‰}$, $\text{Sr} > 200$ ppm, and $\text{Mn}/\text{Sr} < 1.0$. Error bars identify the age correction associated with maximum accumulated error for ^{87}Rb decay, calculated by adding 5% to [Rb], subtracting 5% from [Sr], and adding 5% to age estimate used to calculate correction; average ≈ 0.00002 , range $0.000004\text{--}0.000006$. For Congo data, see footnote 1; Keele peak $^{87}\text{Sr}/^{86}\text{Sr}$ data from Kaufman et al. (1997).

tion) to just beneath the unconformity at the base of the Mulden Group (Hoffmann and Prave, 1996). Two sections, Duurwater and Fransfontein (15°E, 20.2°S), are on the southern (Damara) margin of the craton and about 15 km apart; a third composite section, ~10 km north of the Hoanib River and at Entrance (13.9°E, 19.2°S), is 160 km to the northwest on the western (Kaoko) craton margin. In order to examine interbasinal correlations, high-resolution sampling of glacial and interglacial carbonate units of the Kalahari craton (Hoffmann, 1989; Saylor et al., 1998) and the Amadeus basin, Australia (Preiss, 1987), was carried out. Samples were microdrilled, and Sr, Mn, Fe, Ca, and Mg abundances were measured by using inductively coupled plasma emission spectroscopy to assess diagenetic alteration. Samples were analyzed offline for $\delta^{13}\text{C}$ and $\delta^{18}\text{O}$ after digestion for 3 hours in H_3PO_4 at 50 °C to insure complete reaction of dolomite; the evolved gas was measured on a Finnigan Mat 250 with external precision of 0.1‰ for $\delta^{13}\text{C}$ and 0.5‰ for $\delta^{18}\text{O}$. Some samples with $\text{Mn}/\text{Sr} < 1.5$, $\text{Sr} > 200$ ppm, and $\delta^{18}\text{O} > -6\text{‰}$ were analyzed for $^{87}\text{Sr}/^{86}\text{Sr}$ on a Fisons Sector mass spectrometer (eight runs of NBS 987 averaged 0.710246; analytical uncertainty was ± 0.000009). Rb and Sr were analyzed by graphite-furnace atomic absorption spectroscopy. Samples were leached in $\text{NH}_4\text{CH}_3\text{COO}$ to reduce contamination from radiogenic Sr adsorbed to clays, and then digested for 10 minutes

in weak (<5%) acetic acid. Analytical results are available in Appendix 1.¹

Retention of primary marine $^{87}\text{Sr}/^{86}\text{Sr}$ values is optimized because of the purity and thickness of the Congo carbonate succession, which limited potential contamination from radiogenic Sr in silt and clay during diagenesis. Samples considered least altered (filled circles, Fig. 1) have $\text{Sr} > 200$ ppm (average 865), $\delta^{18}\text{O} > -7\text{‰}$, $\text{Mn}/\text{Sr} < 1.0$, no correlation between $^{87}\text{Sr}/^{86}\text{Sr}$ and Sr/Ca, Fe, or $\delta^{18}\text{O}$.

Five numbered benchmarks in the Congo craton $\delta^{13}\text{C}$ profiles are shown in Figure 1: (1) $\delta^{13}\text{C}$ values rise by ~8‰ from -2‰ within the lower (Rasthof) cap carbonate, (2) there is an interglacial $\delta^{13}\text{C}$ peak of $>+8\text{‰}$ (Keele peak), (3) values decline from $>8\text{‰}$ to $+2\text{‰}$ below a sequence boundary underneath the upper (Ghaub) glacial succession,² (4) they fall monotonically from -1‰ to -5‰ within the upper (Keilberg) cap carbonate and then rise to positive values (1‰–2‰) in overlying late transgressive and early highstand carbonate grainstones, and (5) there is a positive $\delta^{13}\text{C}$ excursion to $+5\text{‰}$ (Maieberg peak) near the top of the sampled succession at Fransfontein. Minimum $^{87}\text{Sr}/^{86}\text{Sr}$ values of 0.7072–3 were

obtained from bedded micrites within the Ghaub glaciogenic interval. Values rise to 0.7079 in micrities at the top of the glacial unit and persist into conformably overlying beds; they fall slightly to 0.7077 higher in the succession (Fig. 1).

AGE OF THE GLACIAL INTERVALS

The lower glacial interval (Chuoss Formation) has been regarded as Sturtian in age as it overlies a U-Pb date of 746 ± 2 Ma (Hoffman et al., 1996) and contains interbedded ironstones. The upper glacial interval (Ghaub Formation) has also been assigned to the Sturtian (Kaufman et al., 1997; Hoffman et al., 1998b), because $\delta^{13}\text{C}$ values of $>8\text{‰}$, found in younger strata (Kaufman et al., 1991), were thought not to occur above Marinoan glacial horizons. However, very positive $\delta^{13}\text{C}$ values constitute a poor criterion for distinguishing Sturtian from Marinoan glaciations because $\delta^{13}\text{C}$ values of $>8\text{‰}$ are recorded from Terminal Proterozoic carbonates in Australia, China, Oman, and Spitsbergen (Jenkins, 1995; Lambert et al., 1987; Burns et al., 1994; Fairchild and Spiro, 1987). Two, rather than one, exceptionally positive post-Marinoan $\delta^{13}\text{C}$ peaks seem likely (Knoll, 1996).

The $^{87}\text{Sr}/^{86}\text{Sr}$ record provides less ambiguous age constraints than the $\delta^{13}\text{C}$ record because values rise from Sturtian levels of 0.7068 below Marinoan glacial strata, through 0.7080 at the close of this ice age, to >0.7090 during the Cambrian (Fig. 2; Derry et al., 1992; Knoll and Walter, 1992). On the Congo craton, $^{87}\text{Sr}/^{86}\text{Sr}$

¹GSA Data Repository item 9887, is available on request from Documents Secretary, GSA, P.O. Box 9140, Boulder, CO 80301. E-mail: editing@geosociety.org.

²In sections near Fransfontein, including Duurwater (Fig. 1), Hoffman et al. (1998b) report $\delta^{13}\text{C}$ values lower than -4‰ beneath the subglacial unconformity.

values rise from 0.7073 low in the Ghaub glacial interval to 0.7079 in overlying postglacial rocks (Fig. 1). These data indicate a Marinoan age, for the Ghaub glaciation.

Less well resolved is the position of the $>5\%$ $\delta^{13}\text{C}$ excursion above the upper glacial interval (Maieberg peak, Fig. 1) relative to a $+9.5\%$ peak (Fig. 2, left panel) that occurs higher in the stratigraphy several hundred kilometers to the east (Otavi Mountainland; Kaufman et al., 1991). It is likely that the $>+8\%$ values from the Otavi Mountainland represent a second positive peak above the Ghaub glaciation; carbonates containing that peak (Huttenberg Formation) are predicted to have $^{87}\text{Sr}/^{86}\text{Sr}$ ratios of ~ 0.7085 (Fig. 2).

CORRELATION OF THE CONGO CRATON RECORD

The Neoproterozoic succession on the Kalahari craton contains two glacial intervals that are geochemically and geologically similar to those described above (Fig. 2). Although the Kalahari glacial deposits have been considered to be entirely younger than those of the Congo craton (Kaufman et al., 1997; Saylor et al., 1998), correlation of these two pairs of deposits is supported by (1) similar $^{87}\text{Sr}/^{86}\text{Sr}$ ratios of $0.7080 \pm$

0.0001 immediately above the upper glacial interval on both the Congo (Fig. 1) and Kalahari (Fig. 2; Kaufman et al., 1997) cratons, (2) similar declines in $\delta^{13}\text{C}$ from -2% to -5% within the upper cap carbonates in contrast to increases in $\delta^{13}\text{C}$ from -2% to $+7\%$ in the lower cap carbonates of both cratons (Fig. 3), (3) the presence of tubestones at the upper glacial level on both cratons (Hegenberger, 1987), and (4) the occurrence of dark, organic-rich microbial laminites and roll-up structures in both lower cap carbonates.

The strong lithological and geochemical differences between upper and lower glacial intervals that are shared by the Congo and Kalahari cratons are also present in Australian (Preiss, 1987; Kennedy, 1996) and Canadian (Aitken, 1991; Narbonne et al., 1994) successions (Fig. 2). The persistence of these characters in widely separated areas provides an independent way to test global correlations previously based largely on the interregional comparison of $\delta^{13}\text{C}$ excursions (Kaufman et al., 1997).

We tabulated 10 geologic and geochemical attributes from 12 well-studied Neoproterozoic glacial deposits plus an "outgroup," the Carboniferous Wynyard Tillite of Tasmania (Fig. 4). This character matrix was analyzed with the maximum parsimony algorithm of PAUP 3.1.1

(Swofford, 1993). Results show that features tabulated in Figure 4 are sufficient to define two distinct groups of glacial successions. As six deposits from group A (Areyonga, Blaubeker, Chuos, Rapitan, Sturt, Elbobreen) invariably occur beneath deposits from group B (Olympic, Bildah-Tsabisis, Ghaub, Ice Brook, Elatina, Wilsonbreen, respectively) wherever two glacial horizons are present in a single succession, it is believed that these two groups have temporal significance (a coincidental likelihood of this result is $1/2^6$ or 0.016). For example, on the Congo craton the lower glacial interval (Chuos) shares characteristics with Sturtian glacial successions, whereas the overlying Ghaub interval is typically Marinoan in type.

How does the Congo succession fare as a model of Sturtian and Marinoan events when assessed by the geologic and geochemical records of other key successions? In Figure 2, we compare chemostratigraphic records from the Kalahari craton, Australia, and the Mackenzie Mountains, Canada, by using groups A and B of Figure 4 as time surfaces. Although the five isotopic features described above are remarkably widespread, two inconsistent features are present within the Mackenzie Mountains succession: (1) A single $^{87}\text{Sr}/^{86}\text{Sr}$ value of 0.7072 in the Icebrook cap carbonate (Narbonne et al., 1994) contrasts with postglacial values of 0.7080 ± 0.0001

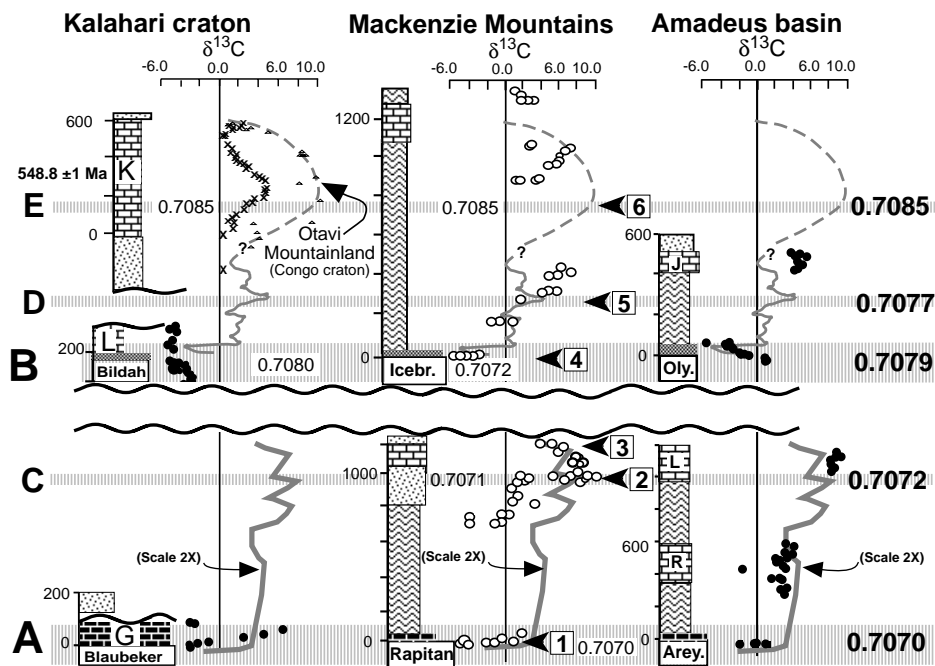


Figure 2. $\delta^{13}\text{C}$ and $^{87}\text{Sr}/^{86}\text{Sr}$ records from key Neoproterozoic sections. $\delta^{13}\text{C}$ data from Figure 1 shown as a five-point running average (gray curves; note $\times 2$ difference in scale in lower panel). Datums A and B correspond to groups shown in Figure 4; datums C, D, and E represent positive $\delta^{13}\text{C}$ excursions (Keele, Maieberg, Huttenberg) and $^{87}\text{Sr}/^{86}\text{Sr}$ values from various sections (Kaufman et al., 1997). Filled symbols—this study; X—U-Pb age (Grotzinger et al., 1995); small triangles (left panel) and dashed gray line—Otavi Mountainland (Kaufman et al., 1991); unfilled circles—(Kaufman et al., 1997). Kalahari craton, Namibia: G—Gobabis Formation, Gobabis; Bildah—Bildah Formation, Okambara (Saylor et al., 1998); L—La Fraque Formation; K—Kubis Subgroup (Saylor et al., 1998). Mackenzie Mountains, Canada: Rapitan—Rapitan Formation; Icebr.—Icebrook Formation; rest undifferentiated Winderemere Group (Kaufman et al., 1997). Amadeus basin, Australia: Arey—Areyonga Formation; R—Ringwood; L—Limbla Members, Aralka Formation; Oly—upper cap carbonate, Olympic Formation, Mount Capitor; J—Julie Formation, Ross River.

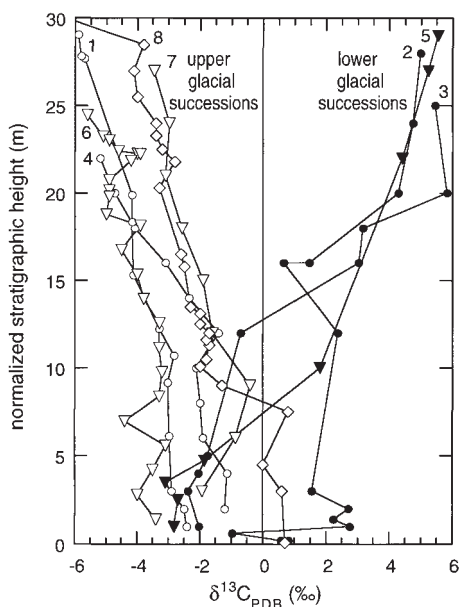
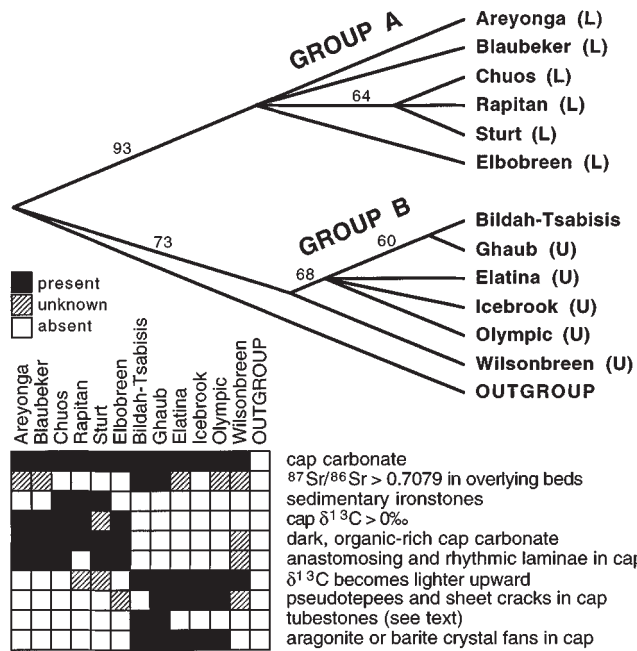


Figure 3. Measured $\delta^{13}\text{C}$ trends within cap carbonates overlying upper (Marinoan; open symbols) and lower (Sturtian; filled symbols) glacial intervals in Congo craton (circles), Kalahari craton (triangles), and Amadeus basin, Australia (diamonds). 1—Fransfontein (15°E , 20.2°S), 2—Duurwater (15.2°E , 20.2°S), 3—Hoanib River (14°E , 19.1°S), 4—Auroos (17.6°E , 19.6°S), 5—Gobabis (19°E , 22.6°S), 6—Okambara (18.1°E , 22.6°S), 7—Blässkrantz (16.2°E , 24.1°S), 8—Mount Capitor (134.6°E , 24°S); thicknesses normalized to 30 m.

Figure 4. Character matrix and strict consensus of seven equally parsimonious trees obtained by using search branch and bound search option of PAUP 3.1.1 (Swofford, 1993); numbers on branches are percent bootstrap support (1000 replicates, heuristic search). A skewness value (g_1) of -0.54 obtained from a sample of 100 000 possible trees demonstrates that data are significantly more structured than random ($P < 0.01$; Hillis and Huelssenbeck, 1992). Sources of non-Congo data: Areyonga (Kennedy, 1996), Blaubeker (Hegenberger, 1987; Saylor et al., 1998), Rapitan (Aitken, 1991), Sturt (Preiss, 1987), Elbobreen (Fairchild and Hambrey, 1995), Bildah-Tsabisis (Hegenberger, 1987; Saylor et al., 1998), Elatina (Preiss, 1987), Icebrook (Aitken, 1991), Olympic (Kennedy, 1996), Wilsonbreen (Fairchild and Hambrey, 1995).



from the Congo and Kalahari cratons, and (2) a pronounced negative $\delta^{13}\text{C}$ excursion, attributed to diagenesis (Kaufman et al., 1997), occurs within the Canadian interglacial interval.

HOW MANY NEOPROTEROZOIC GLACIATIONS?

Except for an event at the Precambrian-Cambrian boundary attributed to ocean overturn (Kimura et al., 1997), no more than two intervals of glaciogenic deposits or impressively negative $\delta^{13}\text{C}$ excursions are established in any single Neoproterozoic succession. Interpretation of more than two glacial intervals and/or negative $\delta^{13}\text{C}$ excursions for this interval relies on the summation of $\delta^{13}\text{C}$ peaks among basins and continents (Kaufman et al., 1997; Saylor et al., 1998). Our results show the following: (1) In a fairly complete succession, only two negative $\delta^{13}\text{C}$ excursions ($\delta^{13}\text{C} < -1\text{‰}$) and associated evidence for glaciation can be identified. (2) Recurrent geochemical and geologic features of Neoproterozoic glacial intervals allow them to be resolved into two distinct groups that are always found in the same stratigraphic order. (3) First-order features of the interglacial and postglacial $\delta^{13}\text{C}$ and $^{87}\text{Sr}/^{86}\text{Sr}$ records are consistent with the hypothesis of only two Neoproterozoic glaciations.

The single possible exception is the occurrence of two glacial intervals on the Varanger Peninsula, Norway (Fairchild and Hambrey, 1984), both considered Marinoan in age (Knoll et al., 1986). Whereas the upper Varanger interval shares close similarities with other Marinoan successions

(Fig. 4; Siedlecka and Roberts, 1992), the age of the lower interval is less well constrained, although an overlying Rb-Sr shale age of 654 ± 23 (Fairchild and Hambrey, 1995) hints at a pre-Marinoan position (Vidal and Moczydlowska, 1995). The principal biostratigraphic constraint is the presence of the microfossil *Balinella faviolata*. Although used as a Vendian (Marinoan) index (Knoll, 1982), its presence in Riphean (Sturtian) successions in Norway (Vidal, 1981) and Utah (Knoll et al., 1981) suggests that more rigorous evidence is needed before this lower Varanger interval is accepted as a third Neoproterozoic ice age. Our analysis suggests it may well be Sturtian (Elbobreen, Fig. 4).

DISCUSSION

The likelihood of only two Neoproterozoic glacial events separated in time by 100–150 m.y. suggests that the glaciations were independent and dominated by factors that operated on tectonic time scales. The rapid rise in seawater $^{87}\text{Sr}/^{86}\text{Sr}$ associated with the Marinoan glacial interval (Fig. 1) after ~100 m.y. of invariant values also favors tectonic drivers, such as enhanced radiogenic runoff from continental weathering following orogenesis or a reduced flux of hydrothermal CO_2 from mantle sources. A similar-magnitude rise in $^{87}\text{Sr}/^{86}\text{Sr}$ also appears to bracket Sturtian glacial deposits (Derry et al., 1992).

The concept of two independent ice ages contrasts with models that call for four or five linked glacial “cycles” (Kaufman et al., 1997). The

latter implies processes operating on shorter time scales, such as variations in organic carbon burial (Knoll et al., 1986). The interglacial decline of $\delta^{13}\text{C}$ values several hundred meters down section from the first evidence for glacioeustatic sea-level fall (Fig. 1) suggests that dominant control on glaciation was not directly linked to processes controlling $\delta^{13}\text{C}$. Positive $\delta^{13}\text{C}$ values in marine carbonates within and immediately overlying Marinoan glaciogenic facies in the Amadeus basin and within the Ghaub Formation (Fig. 2; Kennedy et al., 1997), combined with the return to positive values immediately above the Keilberg cap carbonate (Fig. 1), imply that the negative $\delta^{13}\text{C}$ values are related to cap carbonate precipitation and/or marine transgression rather than to glaciation per se.

An extreme account of the nature of Neoproterozoic ice ages was presented by Hoffman et al. (1998b). Their snowball Earth scenario attributes the extraordinary negative $\delta^{13}\text{C}$ excursion associated with the Ghaub glaciation to an almost complete shutdown of marine biological production. In their model, worldwide sea ice stopped photosynthesis and isolated the oceans from the atmosphere for as long as 10 m.y. Our data are in conflict with this scenario in the following ways: (1) $\delta^{13}\text{C}$ values become positive low in the Maieberg Formation on the southern (Damara) margin of the Congo craton (Fig. 1) in contrast to a 0.5-km-thick $\delta^{13}\text{C}$ excursion that occupies the whole of the Maieberg and much of the overlying Elandshoek Formation on both western (Kaoko) and southern (Damara) sides of the craton (Hoffman et al., 1998b). A prominent sequence boundary at the top of the Maieberg in both areas (sections 4 and 7 of Hoffman et al., 1998a), plus lithological similarities between “platform” and “slope” settings on the Damaran margin, makes extreme condensation of the southern succession unlikely (we prefer a carbonate ramp model for this margin of the craton). It is possible that diagenesis has averaged the carbon isotope compositions of carbonate and organic matter in some Maieberg sections, decreasing the $\delta^{13}\text{C}$ values of the carbonates by several permil; however, we cannot account for the discrepancy between our uniformly positive $\delta^{13}\text{C}$ values beneath the Ghaub Formation at Duurwater (Fig. 1, center panel) and the series of negative values reported by Hoffman et al. (1998b) from the same place and measured thickness (their section 2). (2) Positive $\delta^{13}\text{C}$ values from within the diamictites and cap carbonates in Namibia and Australia (Figs. 2, 3; Kennedy et al., 1997) cannot be explained by the snowball Earth scenario as the oceans are expected to move to mantle compositions (-5‰) when isolated from the atmosphere. (3) The observed shift in marine $^{87}\text{Sr}/^{86}\text{Sr}$ to more radiogenic (continental) values is opposite that predicted by the snowball Earth scenario, which calls for continental runoff to cease during glaciation, resulting in a shift to less radiogenic (mantle) values. In its present form, the snowball Earth sce-

nario fails to account for the most obvious features of the chemostratigraphy of the Congo craton.

The penultimate period of the Neoproterozoic is aptly named the Cryogenian. Its lower boundary is, by definition, exactly 850 Ma (Plumb, 1991). A Subcommittee of the International Commission on Stratigraphy is currently deliberating where to place the GSSP that will separate the Terminal Proterozoic from the Cryogenian. If the GSSP is placed at one of the currently preferred levels (below, within, or above a Marinoan cap carbonate; Knoll and Walter, 1992), then both of the Neoproterozoic ice ages (Sturtian and Marinoan) will lie within the Cryogenian. The next firm evidence for continental glaciation in the geologic record is at the end of the Ordovician.

ACKNOWLEDGMENTS

We thank N. Christie-Blick, R. V. Ingersoll, C. R. Marshall, and G. M. Ross for advice; D. J. Steding for technical assistance; and J. L. Kirschvink, A. H. Knoll, and an anonymous reviewer for helpful comments. The research was funded by the Geological Survey of Namibia, National Science Foundation (grant EAR-9406586 to Prave), and University of California, Los Angeles. IGPP publication no. 5179.

REFERENCES CITED

- Aitken, J. D., 1991, The Icebrook Formation and the post-Rapitan, Late Proterozoic glaciation, Mackenzie Mountains, Northwest Territories: Geological Survey of Canada Bulletin 404, 43 p.
- Burns, S. J., Haudenschild, U., and Matter, A., 1994, The strontium isotopic composition of carbonates from the late Precambrian (560–540 Ma) Huqf Group Oman: Chemical Geology, v. 111, p. 269–282.
- Derry, L. A., Kaufman, A. J., and Jacobsen, S. B., 1992, Sedimentary cycling and environmental change in the Late Proterozoic: Evidence from stable and radiogenic isotopes: *Geochimica et Cosmochimica Acta*, v. 56, p. 1317–1329.
- Fairchild, I. J., and Hambrey, M. J., 1984, The Vendian succession of northeastern Spitsbergen: Petrogenesis of a dolomite-tillite association: *Precambrian Research*, v. 5, p. 111–167.
- Fairchild, I. J., and Hambrey, M. J., 1995, Vendian basin evolution in east Greenland and NE Svalbard: *Precambrian Research*, v. 73, p. 217–233.
- Fairchild, I. J., and Spiro, B., 1987, Petrological and isotopic implications of some contrasting Late Precambrian carbonates, NE Spitsbergen: *Sedimentology*, v. 34, p. 973–989.
- Grotzinger, J. P., Bowring, S. A., Saylor, B. Z., and Kaufman, A. J., 1995, Biostratigraphic constraints on early animal evolution: *Science*, v. 270, p. 598–604.
- Harland, W. B., 1964, Critical evidence for a great Infra-Cambrian glaciation: *Geologische Rundschau*, v. 54, p. 45–61.
- Hegenberger, W., 1987, Gas escape structures in Precambrian peritidal carbonate rocks: Communications of the Geological Survey of South West Africa, Namibia, v. 3, p. 49–55.
- Hillis, D. M., and Huelsenbeck, J. P., 1992, Signal, noise, and reliability in molecular phylogenetic analysis: *Journal of Heredity*, v. 83, p. 189–195.
- Hoffman, P. F., Hawkins, D. P., Isachsen, C. E., and Bowring, S. A., 1996, Precise U-Pb zircon ages for early Damaran magmatism in the Summas Mountains and Welwitschia Inlier, northern Damara belt, Namibia: *Communications of the Geological Society of Namibia*, v. 11, p. 47–52.
- Hoffman, P. F., Kaufman, A. J., and Halverson, G. P., 1998a, Comings and goings of global glaciation on a Neoproterozoic tropical platform in Namibia: *GSA Today*, v. 8, no. 5, p. 1–9.
- Hoffman, P. F., Kaufman, A. J., Halverson, G. P., and Schrag, D. P., 1998b, A Neoproterozoic snowball Earth: *Science*, v. 281, p. 1342–1346.
- Hoffmann, K.-H., 1989, New aspects of lithostratigraphic subdivision and correlation of Late Proterozoic to Early Cambrian rocks of the Damara Belt and their correlation with the central and northern Damara Belt and Gariep Belt: *Communications of the Geological Society of Namibia*, v. 5, p. 59–67.
- Hoffmann, K.-H., and Prave, A. R., 1996, A preliminary note on the revised subdivision and regional correlation of the Otavi Group based on glacial diamictite and associated cap dolostones: *Communications of the Geological Society of Namibia*, v. 11, p. 77–82.
- Jenkins, R. J. F., 1995, The problems and potential of using animal fossils and trace fossils in terminal Proterozoic biostratigraphy: *Precambrian Research*, v. 73, p. 51–69.
- Kaufman, A. J., Hayes, J. M., Knoll, A. H., and Germs, G. B., 1991, Isotopic compositions of carbonates and organic carbon from upper Proterozoic successions in Namibia: Stratigraphic variations and the effects of diagenesis and metamorphism: *Precambrian Research*, v. 49, p. 301–327.
- Kaufman, A. J., Knoll, A. H., and Narbonne, G. M., 1997, Isotopes, ice ages, and terminal Proterozoic earth history: *Proceedings of the National Academy of Sciences*, v. 95, p. 6600–6605.
- Kennedy, M. J., 1996, Stratigraphy, sedimentology, and isotopic geochemistry of Australian Neoproterozoic post glacial cap dolostones: Deglaciation, $\delta^{13}\text{C}$ excursions, and carbonate precipitation: *Journal of Sedimentary Research*, v. 66, p. 1050–1064.
- Kennedy, M. J., Prave, A. R., and Hoffmann, K.-H., 1997, A carbon isotopic record through a Neoproterozoic glacial cycle: *Geological Society of America Abstracts with Programs*, v. 29, no. 6, p. A–196.
- Kimura, H., Matsumoto, R., Kakuwa, Y., Hamdi, B., and Zibaseresh, H., 1997, The Vendian-Cambrian $\delta^{13}\text{C}$ record, north Iran: Evidence for overturning the ocean before the Cambrian explosion: *Earth and Planetary Science Letters*, v. 147, p. E1–E7.
- Kirschvink, J. L., 1992, Late Proterozoic low latitude glaciation: The snowball earth, in Schopf, J. W., and Klein, C., eds., *The Proterozoic biosphere: A multidisciplinary study*: Cambridge, Cambridge University Press, p. 51–52.
- Knoll, A. H., 1982, Microfossil-based biostratigraphy of the Precambrian Hecla Hoek sequence, Nordaustlandet, Svalbard: *Geological Magazine*, v. 119, p. 269–279.
- Knoll, A. H., 1996, Daughter of time: *Paleobiology*, v. 22, p. 1–7.
- Knoll, A. H., and Walter, M. R., 1992, Latest Proterozoic stratigraphy and earth history: *Nature*, v. 356, p. 673–678.
- Knoll, A. H., Blick, N., and Awaramik, S. M., 1981, Stratigraphic and ecological implications of late Precambrian microfossils from Utah: *American Journal of Science*, v. 281, p. 247–263.
- Knoll, A. H., Hayes, J. M., Kaufman, A. J., Swett, K., and Lambert, I. B., 1986, Secular variation in carbon isotope ratios from the upper Proterozoic succession of Svalbard and east Greenland: *Nature*, v. 321, p. 832–839.
- Lambert, I. B., Walter, M. R., Wenlong, Z., Songnian, L., and Guogan, M., 1987, Paleoenvironment and carbon isotope stratigraphy of upper Proterozoic carbonates of the Yangtze Platform: *Nature*, v. 325, p. 140–143.
- Narbonne, G. M., Kaufman, A. J., and Knoll, A. H., 1994, Integrated chemostratigraphy and biostratigraphy of the upper Windermere Supergroup (Neoproterozoic), northwestern Canada: Implications for Neoproterozoic correlations and the early evolution of animals: *Geological Society of America Bulletin*, v. 106, p. 1281–1292.
- Plumb, K., 1991, New Precambrian time scale: *Episodes*, v. 14, p. 139–140.
- Prave, A. R., 1996, A tale of two cratons: Tectonic anatomy of the Damara orogen in northwestern Namibia and the assembly of Namibia: *Geology*, v. 24, p. 115–118.
- Preiss, W. V., 1987, The Adelaide geosyncline—Late Proterozoic stratigraphy, sedimentation, paleontology, and tectonics: *Geological Society of South Australia Bulletin* 53, 438 p.
- Saylor, B. Z., Kaufman, A. J., Grotzinger, J. P., and Urban, F., 1998, The partitioning of terminal Neoproterozoic time: Constraints from Namibia: *Journal of Sedimentary Research* (in press).
- Schmidt, P. W., and Williams, W. E., 1995, The Neoproterozoic climatic paradox: Equatorial paleolatitude for Marinoan glaciation near sea level in South Australia: *Earth and Planetary Science Letters*, v. 134, p. 107–124.
- Siedlecka, A., and Roberts, D., 1992, The bedrock geology of Varanger Peninsula, Finmark, north Norway: An excursion guide: *Norges Geologiske Undersøkelse Special Publication* 5, 45 p.
- Swofford, D. L., 1993, PAUP: Phylogenetic analysis using parsimony. Version 3.1.1: Champaign, Illinois Natural History Survey.
- Vidal, G., 1981, Micropaleontology and biostratigraphy of the upper Proterozoic and Lower Cambrian sequences in East Finmark, northern Norway: *Norges Geologiske Undersøkelse*, v. 362, p. 1–53.
- Vidal, G., and Moczydlowska, M., 1995, The Neoproterozoic of Baltica—Stratigraphy, palaeobiology, and general geological evolution: *Precambrian Research*, v. 73, p. 197–216.

Manuscript received July 10, 1998

Revised manuscript received August 28, 1998

Manuscript accepted September 8, 1998